Hindawi
International Journal of RF and Microwave Computer-Aided Engineering
Volume 2023, Article ID 1668006, 13 pages
https://doi.org/10.1155/2023/1668006

Research Article

Mitigating Thermal Focusing in Microwave Heating of Cylindrical Loads by Resonant Rings

Fengming Yang,[1] Xueting Yan,[1] Huacheng Zhu,[1,2] Yang Yang,[1,2] and Kama Huang[1]

[1]*College of Electronics and Information Engineering, Sichuan University, Chengdu 610065, China*
[2]*Tianfu Engineering-oriented Numerical Simulation & Software Innovation Center, Chengdu 620107, China*

Correspondence should be addressed to Yang Yang; yyang@scu.edu.cn

Received 31 July 2023; Revised 14 September 2023; Accepted 9 October 2023; Published 25 October 2023

Academic Editor: Piotr Gas

Cylindrical loads are commonly found in microwave heating. However, cylindrical loads tend to have a thermal focus, leading to uneven microwave heating. In this paper, a novel microwave heating method was proposed by employing resonant rings to mitigate the thermal focus of cylindrical loads. Firstly, a multiphysics simulation model for microwave heating of a cylindrical tube is established, and the influence of the resonant ring around the cylindrical tube on the temperature distribution of load was analyzed. Subsequently, microwave heating experiments of agar gels with and without resonant rings were carried out. In agreement with the simulation results, the use of resonant rings reduces the coefficient of temperature variation (COV) from 1.064 to 0.793. In addition, the parameters affecting the heating uniformity of the cylindrical tube were discussed through simulations.

1. Introduction

Microwave as green energy was used in various industries due to its numerous advantages, including selective heating, volumetric heating, and low thermal inertia [1–3]. Cylindrical loads are commonly found in microwave heating applications, such as continuous flow tubes in industrial production and cylindrical containers in domestic microwave ovens [4, 5]. Especially in industrial production, the materials to be heated are often subjected to continuous flow heating in cylindrical tubes, thereby ensuring enhanced production efficiency [6]. However, the shape of the load can affect the uniformity of microwave heating. Fia and Amorim conducted numerical simulations to evaluate the heating efficiency and uniformity of wood, bagasse, orange peel, and palm oil in a microwave oven [7]. They investigated how the shape and size of the samples, whether cylindrical or spherical, affect microwave heating. This work is both meaningful and valuable as it provides quantitative evidence for the influence of sample dimensions on microwave heating performance. Zhang and Datta conducted numerical computations and observed that food in a cylindrical container tends to heat up primarily at the center [8]. Soto-Reyes et al. also supported this finding by demonstrating the thermal focusing phenomenon in cylindrical loads when heating various shapes of loads [9]. Such uneven heating presents serious problems in production. For example, in food production, there is a microbial risk when food is incompletely heated, and excessive heating may cause serious nutrient loss [10–12]. Therefore, it is of great significance to improve the uniformity of continuous flow microwave heating for food production.

The microwave heating characteristics of cylindrical loads were studied. It is found that microwave frequency, cylinder radius, heat transfer, permittivity, and heat transfer coefficient all affect the uniformity of microwave heating [13, 14]. Therefore, there are various ways to improve the uniformity of microwave heating. The most common method is mode stirring, which uses a metal or dielectric stirrer in the cavity to continuously change the mode of the electromagnetic field during heating. It is also possible to move the feed source or loads during the heating, which is also

the same principle [15–18]. However, mode stirring will affect the microwave heating efficiency, and the effect is not obvious for large-volume loads, because the influence of the shape of the load on the electromagnetic field distribution is often dominant. At present, some methods have been proposed to improve the uniformity of microwave heating and prevent excessive temperature differences in the heated samples. Li et al. designed a single-mode traveling-wave reactor for microwave heating, and this reactor tries to maintain single-mode microwave propagation to improve microwave uniformity [19]. Bhattacharya and Basak investigated how container material affects microwave heating of cylindrical loads. They proposed using a lossy container to improve heating uniformity by altering the electric field distribution [20]. Their latest research also found that the thickness of the container affects the pattern of the electromagnetic field in the load, which affects the efficiency and uniformity of heating [21]. Tuta et al. found that the use of a helical tube in microwave heating systems can achieve more uniform heating [22]. Coskun et al. proposed a cylindrical tube microwave heating system for industrial production, employing different insulation tubes to overcome the unevenness of heating [23]. Zhu et al. presented a microwave heating system that was carried out with a screw propeller for continuous flow processing to realize uniform temperature distribution [24]. Xu et al. applied a leaky waveguide in a continuous flow microwave reactor to obtain a uniform distribution of microwave energy [25]. However, the above studies concentrated on replacing the components of the microwave heating system, such as improving waveguides or using spiral tubes. In fact, cylindrical tubes are ideal and convenient containers for continuous production, and they have the advantages of simple structure, large capacity, and easy processing, but the problem of inhomogeneity and thermal focusing caused by cylindrical loads has not yet been solved.

To solve the heating inhomogeneity mentioned above, a microwave heating system with resonant rings surrounding the surface of a cylindrical tube is presented. The use of the resonant ring changes the propagation path of the electromagnetic wave incident on the cylindrical load, which can alleviate the thermal focus during heating. Additional electromagnetic field modes are generated in the cylindrical load by resonance, thereby improving the uniformity of heating. In Section 2, a multiphysics simulation model is established, and a resonant ring that can improve uniformity is designed. In Section 3, the model is verified by experiments, and the influence of loading parameters on the heating uniformity is discussed.

2. Methodology

2.1. Method of Resisting Thermal Focusing. When the microwave propagates through the curved surface of the cylinder, it will generate a central focus inside the cylinder. In the focusing process, the transmitted wave will converge to a smaller volume within the material. Microwave focusing is related to the penetration depth as well as the wavelength, and the penetration depth and wavelength are intermediate parameters that affect the electromagnetic field mode. The relationship between wavelength λ, penetration depth L, and dielectric properties is shown below [26]:

$$\lambda = \frac{2\pi}{\beta}, \qquad L = \frac{1}{2\alpha}, \tag{1}$$

where [26]

$$\alpha = \frac{\sqrt{2}\pi f}{c}\sqrt{\sqrt{\varepsilon'^2 + \varepsilon''^2} - \varepsilon'}, \qquad \beta = \frac{\sqrt{2}\pi f}{c}\sqrt{\sqrt{\varepsilon'^2 + \varepsilon''^2} + \varepsilon'}. \tag{2}$$

The ε' is the real part of relative permittivity, f is the frequency, and c is the speed of light. ε' and ε'' are related to the heating concentration and play an important role.

Thermal focusing inside a cylinder can be explained by the plane wave propagation in the cross-section of the cylinder, as shown in Figure 1. The plane wave propagates in the positive direction along the z axis and is incident from the boundary of a circle with the angle of incidence θ_i. The transmission angle θ_t is obtained from Snell's law [27]:

$$\frac{\sin\theta_i}{\sin\theta_t} = \sqrt{\frac{\varepsilon_{rem}}{\varepsilon_{rin}}}, \tag{3}$$

where ε_{rem} is the relative permittivity outside the circle and ε_{rin} is the relative permittivity inside the circle. The intersection position of the refracted wave and the central axis along the z direction is [27]

$$z = a\frac{\eta}{1-\eta^2}\left(\sqrt{1-\eta^2\sin^2\theta_i} + \eta\cos\theta_i\right), \tag{4}$$

where a is the radius of a cylindrical tube and $\eta = (\varepsilon_{rin}/\varepsilon_{rem})^{0.5}$. The energy concentration location is related to $\varepsilon_{rin}/\varepsilon_{rem}$ and the radius of the cylindrical tube.

If other objects are placed outside the tube, it is equivalent to changing the $\varepsilon_{rin}/\varepsilon_{rem}$, so it will change the position of the hot spot and avoid the central heat focus. By placing metal resonant rings around the tube, the microwave is incident on the resonant ring, and it will be reflected, which can weaken the focus of the microwave energy. Moreover, the resonance of the resonant ring produces more electromagnetic field modes, which can effectively improve the uniformity of heating.

2.2. Modeling

2.2.1. Geometry. In this paper, a microwave heating model is built using COMSOL Multiphysics software (6.0 COMSOL Inc., Stockholm, Sweden), as shown in Figure 2. This system included a rectangular heating cavity, WR340 waveguide,

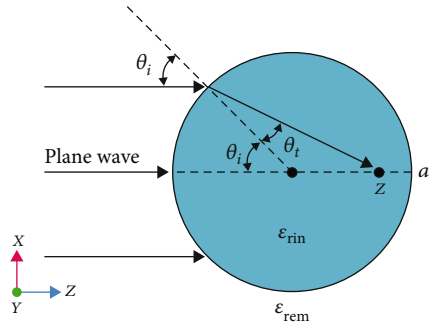

FIGURE 1: Schematic diagram of plane wave incident on the cylinder [27].

cylindrical tube made of quartz, and resonant rings made of aluminum. The cylindrical tube and rectangular microwave cavity are combined into a continuous flow microwave heating system. The cylindrical tube is placed on the central axis of the rectangular cavity, and the length of the tube is exactly equal to the length of the cavity. The WR340 waveguide is connected to the rectangular heating cavity as a power feed port, and the input microwave power at the port is 500 W with a frequency of 2.45 GHz. To observe the temperature distribution of the cylindrical load, a nonflowing agar gel was used as the heated load.

2.2.2. Governing Equation. In this model, the electromagnetic field and solid heat transfer are coupled within the cavity, and Maxwell's equations are used to calculate the internal electromagnetic field [16].

$$\begin{aligned} \nabla \times \vec{H} &= \vec{J} + \varepsilon \frac{\vec{H}}{\partial t}, \\ \nabla \times \vec{E} &= -\mu \frac{\vec{H}}{\partial t}, \\ \nabla \cdot \vec{B} &= 0, \\ \nabla \cdot \vec{D} &= \rho_c, \end{aligned} \tag{5}$$

where $\vec{H}$ is the magnetic field intensity (A/m), $\vec{J}$ is the current density (A/m^2), ε is the relative permittivity, $\vec{E}$ is the electric field intensity (V/m), t denotes the time (s), μ is the magnetic field permeability (H/m), $\vec{B}$ is the magnetic induction strength (T), $\vec{D}$ is the electric displacement vector (C/m), and ρ_c is the charge density (C/m^2).

Electromagnetic energy loss in the microwave heating process is the heat source, which is expressed by the following equation [16]:

$$Q_e = \frac{1}{2}\omega \varepsilon_0 \varepsilon'' \left|\vec{E}\right|^2, \tag{6}$$

where Q_e is the electromagnetic energy loss, ω is the microwave angular frequency, and ε_0 is the vacuum permittivity. The temperature distribution of the heated samples is calculated by the following heat transfer equation [16]:

$$\rho C_\rho \frac{\partial T}{\partial t} - K_t \nabla^2 T = Q_e, \tag{7}$$

where ρ is the density of the substance, C_ρ is the atmospheric heat capacity of the substance (J/kg·K), K_t is the thermal conductivity of the substance (W/m·K), and T indicates the temperature. Based on the above equation, the temperature distribution of the heating model can be calculated.

2.2.3. Input Parameter. Table 1 presents the relevant parameters of the materials used in the simulation [28]. The agar gel serves as the heated sample for measuring temperature variations at different points. The material parameters of air and aluminum use the built-in parameters of COMSOL software, and the relative permeability of all materials is 1.

2.2.4. Boundary Conditions. The surface of the whole waveguide and the whole rectangular heating cavity is assumed to be perfect electrical conductors (PEC). At the waveguide port, it is set to waveport excitation, and the electromagnetic wave mode is TE_{10}. The material of the resonant rings is aluminum. Electromagnetic waves will undergo total reflection on metal surfaces, and the conditions are as follows:

$$\begin{aligned} \vec{e}_n \times \vec{E}_1 &= 0, \\ \vec{e}_n \times \vec{H}_1 &= \vec{J}_s. \end{aligned} \tag{8}$$

Quartz and agar gel are media, and electromagnetic waves will be reflected and incident on their surfaces, and the conditions are as follows:

$$\begin{aligned} \vec{e}_n \times \left(\vec{E}_1 - \vec{E}_2\right) &= 0, \\ \vec{e_n} \times \left(\vec{H}_1 - \vec{H}_2\right) &= 0, \end{aligned} \tag{9}$$

where $\vec{e}_n$ is the normal unit vector of the interface, $\vec{E}_1$ and $\vec{E}_2$ are the electric field strengths on both sides of the interface, $\vec{H}_1$ and $\vec{H}_2$ are the magnetic field strengths on both sides of the interface, and $\vec{J}_s$ is the surface current distribution.

For the thermal boundary, the external surface temperature is well below the internal temperature of the cylindrical sample during heating, and the heating concentration inside the cylindrical sample is the main concern, so the heat transfer between the air and tube can be ignored, and their boundary conditions are set as thermal insulation.

2.2.5. Mesh Setting. When constructing the mesh, an appropriate mesh size should be selected. A mesh size that is too precise and used with insufficient computation memory will lead to a long computation time for model simulation, while a mesh size that is too coarse will lead to inaccurate model

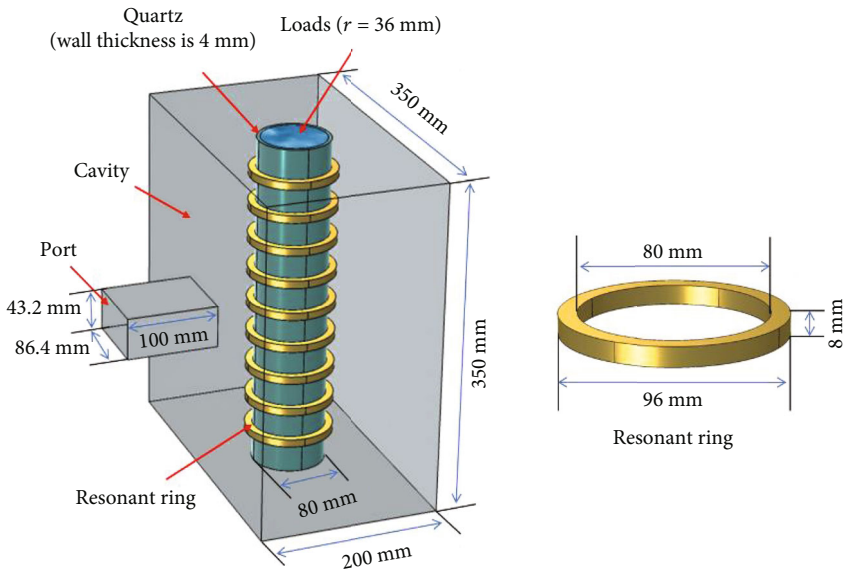

Figure 2: Geometry of the 3D simulation model (the number of resonant rings is 9).

Table 1: Input parameter.

Property	Physical	Value	Source
Real part of relative permittivity	Quartz	4.2	COMSOL built-in
	Agar gel	$78.84 - 6.45 \times 10^{-2} T - 2.38 \times 10^{-3} T^2$	Ref. [28]
Imaginary part of relative permittivity	Quartz	0	COMSOL built-in
	Agar gel	$19.34 - 0.406T + 2.68 \times 10^{-3} T^2$	Ref. [28]
Density (kg/m^3)	Quartz	730	COMSOL built-in
	Agar gel	1000	Ref. [28]
Thermal conductivity (W/m·K)	Quartz	1.4	COMSOL built-in
	Agar gel	0.558	Ref. [28]
Specific heat capacity (J/kg·K)	Quartz	730	COMSOL built-in
	Agar gel	4206	Ref. [28]

simulation results. Studying the independence of the grid can effectively avoid the above problems. Normalized power absorbed (NPA) is used in carrying out mesh independence studies. It is expressed as follows [29]:

$$\mathrm{NPA} = \frac{\text{power absorbed by material}}{\text{power fed into system}}. \tag{10}$$

If the NPA gradually becomes a stable value even the number of grids increases, it means that the simulation results are accurate and no longer affected by the number of mesh elements. According to the simulation model, a mesh composed of 93811 tetrahedral elements in total (having 24608 elements in continuous flow heating) is selected for calculation, as shown in Figure 3.

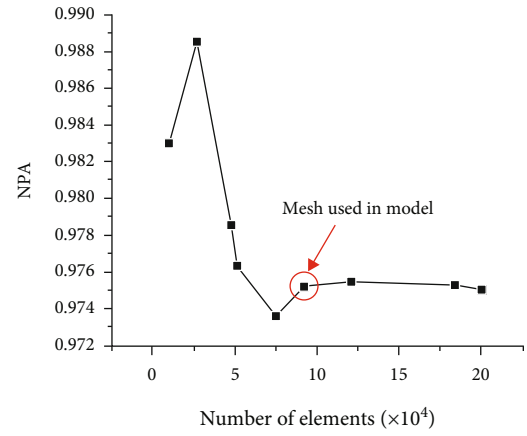

Figure 3: Mesh independence study.

The computational facility employed for our simulations was a DELL XPS 8950 computer equipped with an Intel Core i9-12900K Processor (3.9 GHz, 16 Cores), 64 GB of DDR5 memory running at 4400 MHz, a 1 TB PCIe SSD for storage, and an 8 GB NVIDIA GeForce RTX 3060 Ti graphics card. The operating system used was Windows 11 (21H2). These hardware specifications ensured that our simulations were conducted efficiently and effectively, providing the computational power required for our research.

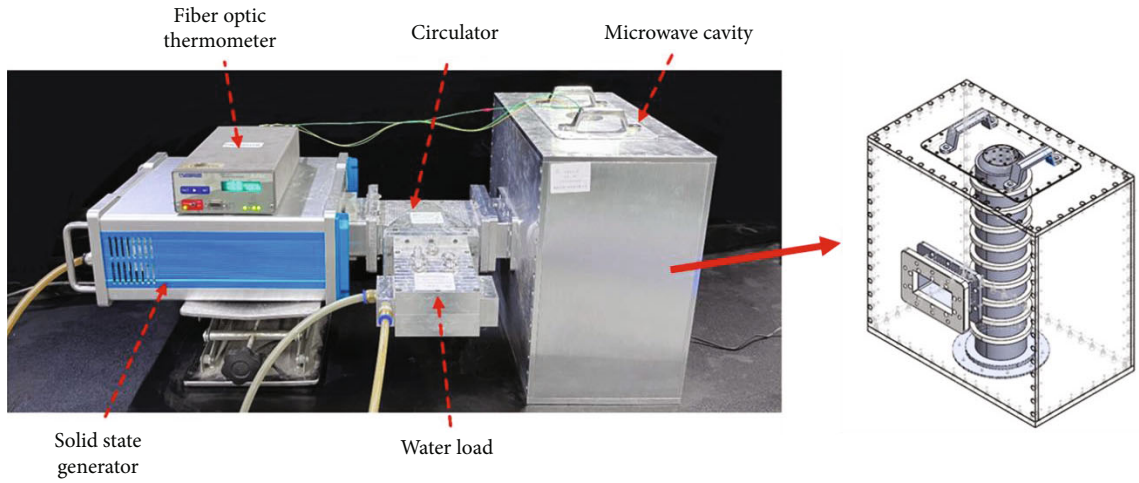

Figure 4: Microwave heating experimental system.

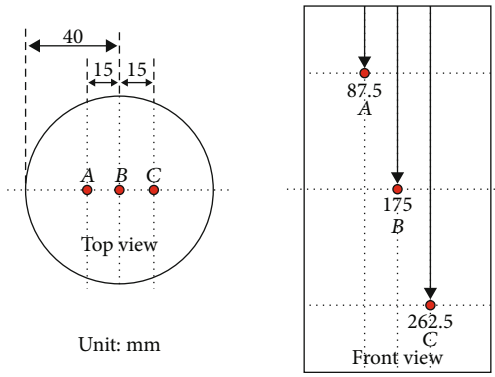

Figure 5: Measurement points for the temperature increase.

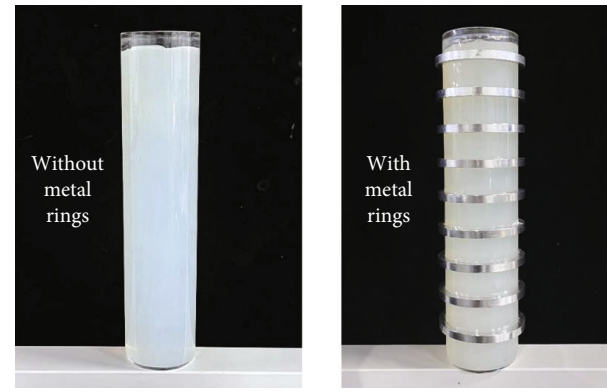

Figure 6: Prepared agar gel sample.

2.3. Experimental Setup

2.3.1. Measurement System. An experiment of microwave heating agar gel was carried out to verify the simulation model. The top surface of the microwave cavity is provided with a rectangular cover for material placement and removal, the rectangular lid contains a circular lid with five small holes used for measuring the temperature of the material, and the groove structure on the bottom of the cavity ensures that the material can be placed in the same position during each experiment. Figure 4 shows the entire experimental system. In addition to the heating cavity, it also includes a solid-state source, circulators, power meter, fiber optic thermometer (FISO FOT-NS-967A, FISO Technologies, Quebec, Canada), and water load.

The solid-state generator was used to provide 500 W input power at a frequency of 2.45 GHz, and circulators and the water load were employed to protect the solid-state generator. The temperature increase shown in Figure 5 at points A, B, and C was measured by a fiber optic thermometer. Considering that an excessively long heating time will cause the solid-state agar gel to melt, the heating time here is 90 s.

2.3.2. Sample Preparation. The dielectric properties of agar gel with high moisture content are very close to those of water, and agar gel is convenient for temperature measurement, so agar gel was used for the experiments. 20 g of agar powder was stirred with a small amount of cold water to form a paste, and 2000 ml of cold water was heated to 100°C in an oil bath. Then, the paste was poured into the oil bath under constant stirring until the agar powder was completely dissolved. Next, the agar solution was poured into a quartz tube customized according to the simulation model, cooled to room temperature, and formed into a solid cylindrical sample, as shown in Figure 6.

3. Results and Discussion

3.1. Experimental Validation. To verify the accuracy of the simulation, the experimental temperature increase at the three points measured by the fiber optic thermometer is compared with the simulated temperature increase after 90 s of microwave heating, and the temperature increase of the same point in the tube with and without resonant rings is compared, as shown in Figure 7. Point B is the center point of the cylindrical sample, and the temperature increase at point B is the highest because the cylindrical sample has a thermal focus, which is observed in both the experimental and simulation results. However, it can be seen that the temperature increase of the cylindrical tube with resonant rings

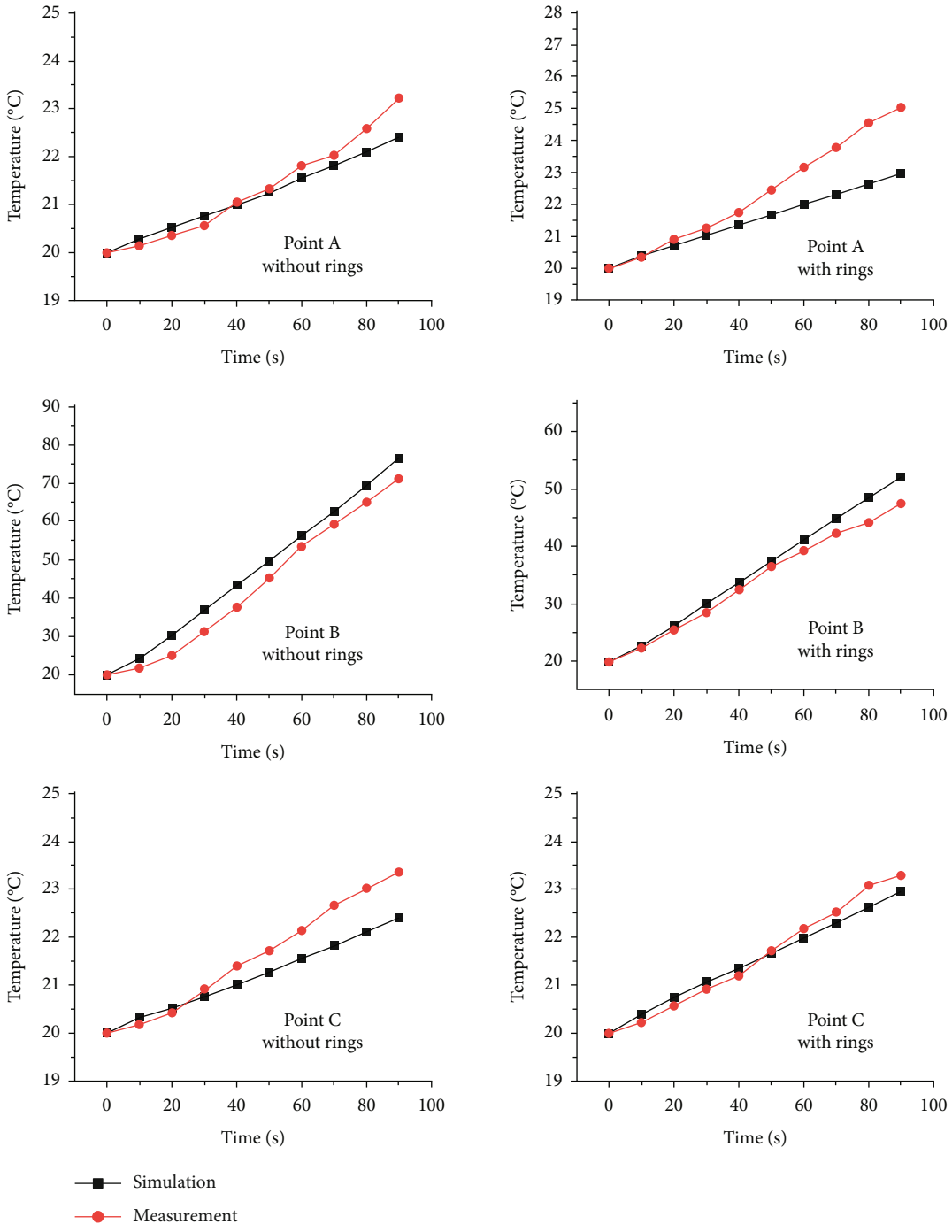

Figure 7: Temperature curve at different points.

at point B is much lower than that without resonant rings. The temperature increase at point A and point C is not much different when the tube has resonant rings and when the tube does not have resonant rings. The experimental and simulation results show a similar temperature rise trend with slight temperature errors. It shows that the simulation model is correct. There are some errors in experiments and simulations, which are more obvious at points A and C. Several potential sources of error exist in both simulations and experiments. These include differences in the relative permittivity of the agar gel in the real-world compared to our simulation settings, simplifications in the simulation model regarding natural convection and cavity wall roughness, deviations in the measurement position of the fiber optic thermometer, and the impact of processing errors in the cavity, quartz tube, and metal ring on our experimental results.

3.2. Hot Spot Analysis. The thermal focusing of the load under the microwave field can be analyzed by the above simulation model. It is known from the analysis of plane waves that the thermal focus of the cylindrical loads depends on the permittivity and the diameter of the tube. To determine

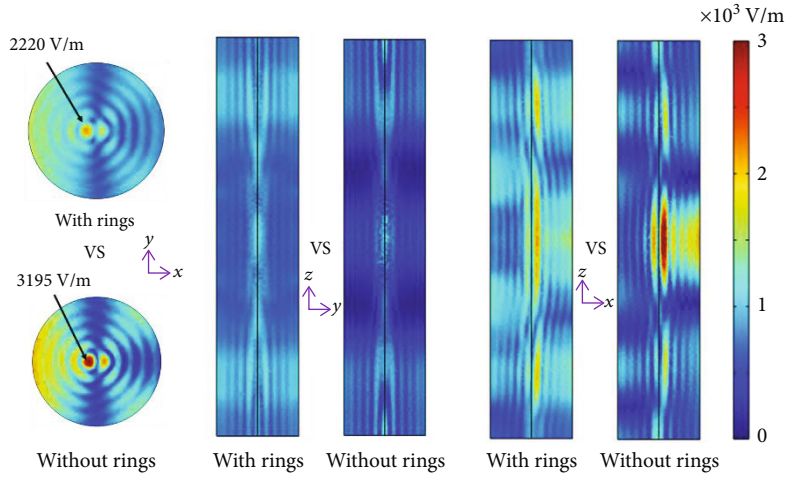

FIGURE 8: Comparison of the electric field distribution in the central cross-section of the cylindrical load.

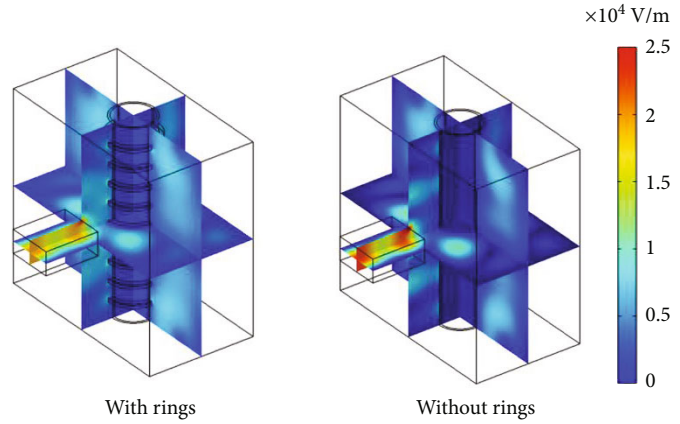

FIGURE 9: Comparison of the electric field distribution in the cavity.

the location of the focusing of the electric field in a cylindrical load, the electric field distribution was simulated for the central cross-section of the agar gel at 20°C along the x, y, and z axes.

Figure 8 shows the electric field distribution in the central cross-section of the cylindrical load with and without resonant rings. It can be seen that the maximum electric field intensity appears at the center point; that is, cylindrical loads exhibit strong central focusing of the electric field. The use of the resonant ring cannot completely avoid the focusing of energy, but it can weaken the focusing of the electric field and make the electric field distribution more uniform. The electric field distribution in the cavity is shown in Figure 9. It can be seen that the resonant ring does not change the distribution of the main electric field modes but generates high-order electromagnetic field modes around the resonant ring, making the electric field distribution in the cavity more uniform.

The relative permittivity of the agar gel changes with temperature, and the variation of S_{11} over time during the heating is depicted in Figure 10. S_{11} is the reflection coefficient of the signal at port 1. S_{11} refers to a parameter commonly used to describe the reflection characteristics of a

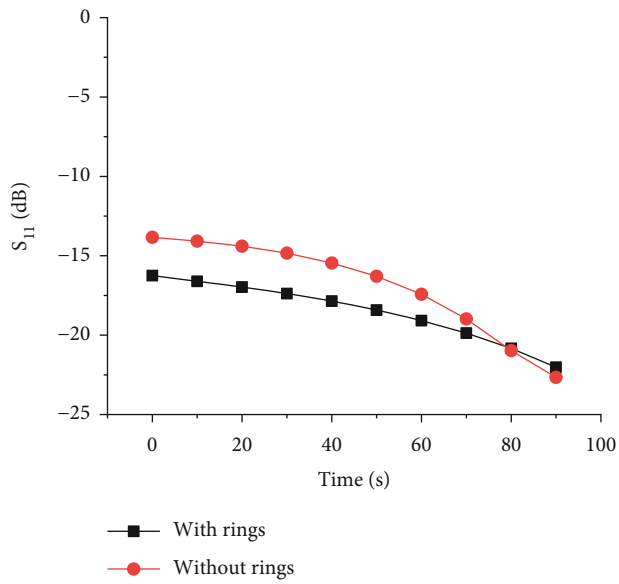

FIGURE 10: The S_{11} curves at different times with and without resonant rings.

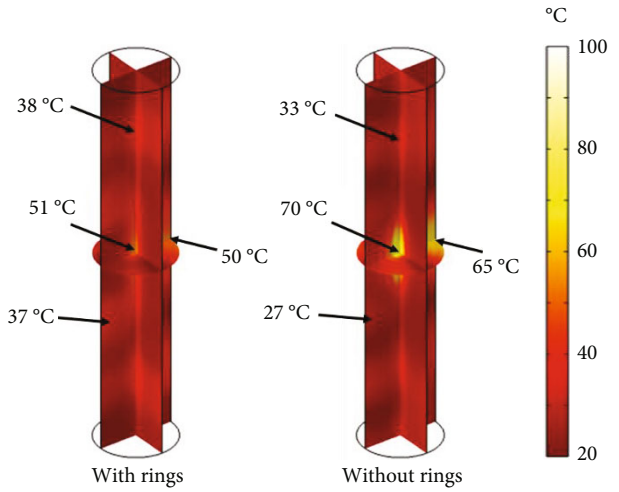

Figure 11: Temperature distribution of cylindrical load with and without resonant ring.

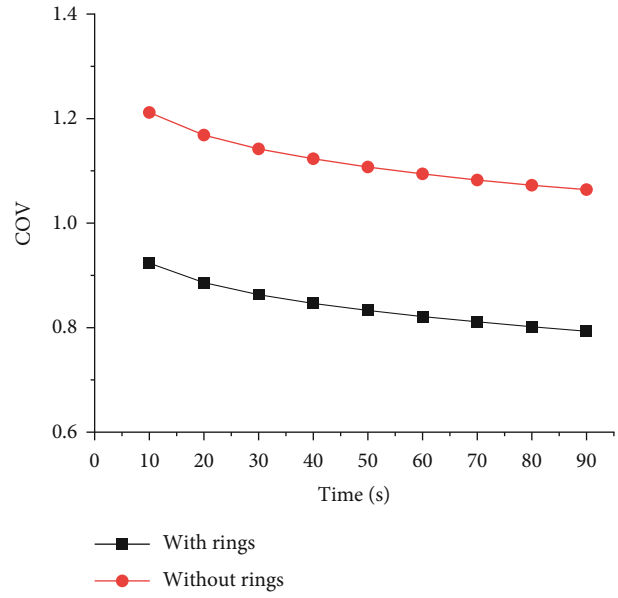

Figure 12: Comparison of COV curves with and without the resonator rings.

Table 2: Comparison of simulation results.

Methods	Average body temperature	COV
With rings	27.39°C	1.064
Without rings	27.32°C	0.793

circuit or antenna. In microwave heating, S_{11} is used to assess the matching between the microwave source and the heated sample. When the absolute value of S_{11} is high, it indicates higher energy efficiency, whereas S_{11} approaching zero suggests greater reflection. In the whole microwave heating system, only the cylindrical load has an electromagnetic loss, so the value of S_{11} can be used to evaluate the microwave heating efficiency. In the experiment, the power absorption efficiency during heating was measured using a power meter and directional coupler. The directional coupler was connected between the cavity and the circulator. During the heating, the input power was maintained at 500 W. The reflected power gradually decreased, with the reflected power being roughly the same for both cases with and without the resonator ring, ranging from approximately 10 W to 50 W. Indeed, it can be observed that throughout the entire heating process, both microwave systems maintain an energy efficiency of 95% or higher.

The temperature distribution of the agar gel heated for 90 s was simulated, and the comparison of the heating results with and without rings is shown in Figure 11. From the simulation results, it can be seen that the use of the resonant ring makes the temperature distribution inside the cylindrical load more uniform so that the hot and cold spots are not sharp. The central region of the cylinder has the most pronounced hot spot, which was reduced by 21°C using the resonant ring. Moreover, the range of hot spots has been significantly reduced.

In this paper, the coefficient of variation (COV) is employed to measure the uniformity of the temperature distribution. It is the standard deviation to mean ratio and can be expressed as [29]

$$\mathrm{COV} = \frac{\sum_{i=1}^{n}(Ti - T_a)^2/n}{(Ta - T0)}, \tag{11}$$

where Ti is the point temperature, T_a is the average temperature, n is the total number of points in the selected area, and $T0$ is the initial average temperature. The smaller the value of COV is, the better the temperature uniformity. The curves depicting the change in COV over time with and without the resonator rings are shown in Figure 12. The average body temperature and COV of the cylindrical load were calculated for the two heating methods, as shown in Table 2. There was little difference in average body temperature between the two methods, but the COV was reduced by 25% using the resonant rings.

3.3. Effect of the Parameter of Resonant Rings on the Heating Performance. Various numbers (N) of resonant rings are analyzed, and their positions vary with the number of resonant rings. The other parameters of the resonant rings are not changed, as shown in Figure 13. During the simulation, five different values of N are studied in the same simulation process, which are 2, 4, 5, 6, and 9. Therefore, the distance (D) between resonant rings in five different setting processes is 87.5 mm, 70 mm, 58.33 mm, 50 mm, and 35 mm. In the simulation, the distance between the resonant rings is equal to the distance between the resonant rings and the cavity.

The simulation results showing the temperature distribution of the cylindrical load with different ring distances are shown in Figure 14. The use of the resonant ring reduces the temperature in the central area of the load. When the number of resonant rings is 3, 4, and 5, there is still an obvious hot spot in the central area of the cylindrical load. When the number of resonant rings reaches 6, the hot spot in the central area of the cylindrical load is no longer obvious.

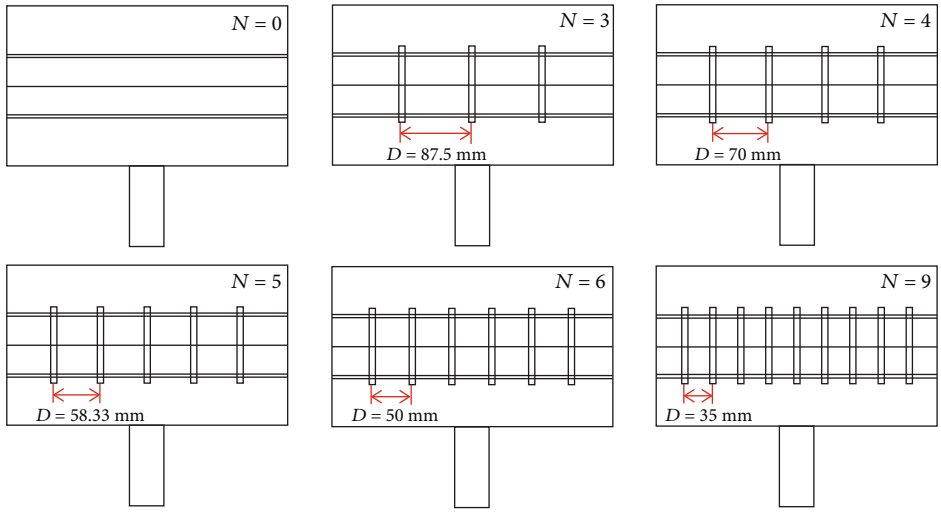

Figure 13: Number of resonant rings and the distance between resonant rings.

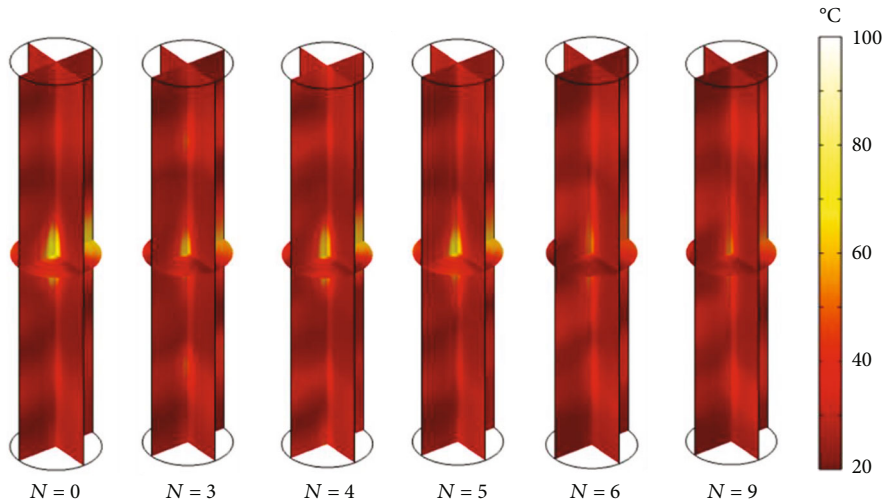

Figure 14: Temperature distribution for different numbers of resonant rings.

When using 9 resonant rings, not only does the hot spot in the center disappear, but the temperature distribution in other areas also becomes more uniform.

Table 3 gives the S_{11} and COV values with different ring distances. It can be seen that the use of the resonant ring has little effect on the average volume temperature of the load but can significantly affect the COV. When the number of resonant rings reaches 6, the COV decreases from 1.064 to 0.828. When the number of resonant rings reaches 9, the COV reaches 0.793, and there is no obvious hot spot in the cylindrical load. Therefore, the best heating uniformity was obtained when the number of resonant rings was 9 and the distance was 3.50 mm.

3.4. Effect of the Parameter of Loads on the Heating Performance. The thermal focus of cylindrical loads has a strong dependence on the radius of the cylindrical load. The S_{11} and the COV of cylindrical loads (agar gel) with different radii were analyzed, both with and without resonant rings. The radii of the cylindrical loads varied from 20 mm to 50 mm in 5 mm increments, and the simulation results are depicted in Figure 15. In the simulation, we changed the radius of the load, the wall thickness of the quartz tube always remained 4 mm, the number of resonant rings was 9, and the axial and radial dimensions of the resonant ring were both 8 mm. The inner wall size of the quartz tube and

Table 3: S_{11} and COV of cylindrical tubes with different distances.

Number	Distance	Temperature (°C)	COV
0	0 mm	27.323	1.064
3	87.5 mm	27.359	0.879
4	70 mm	27.285	0.935
5	58.33 mm	27.313	0.932
6	50 mm	27.348	0.828
9	35 mm	27.394	0.793

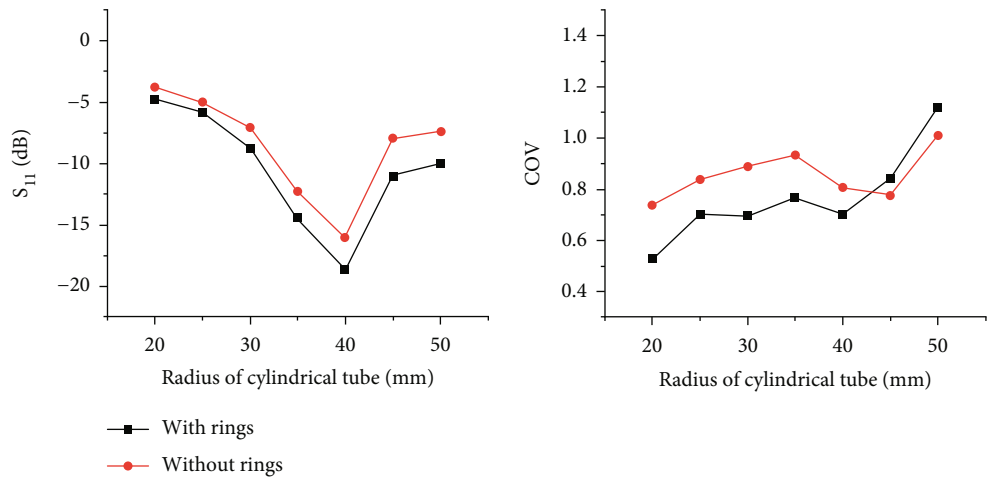

FIGURE 15: The results of S_{11} and COV at different radii.

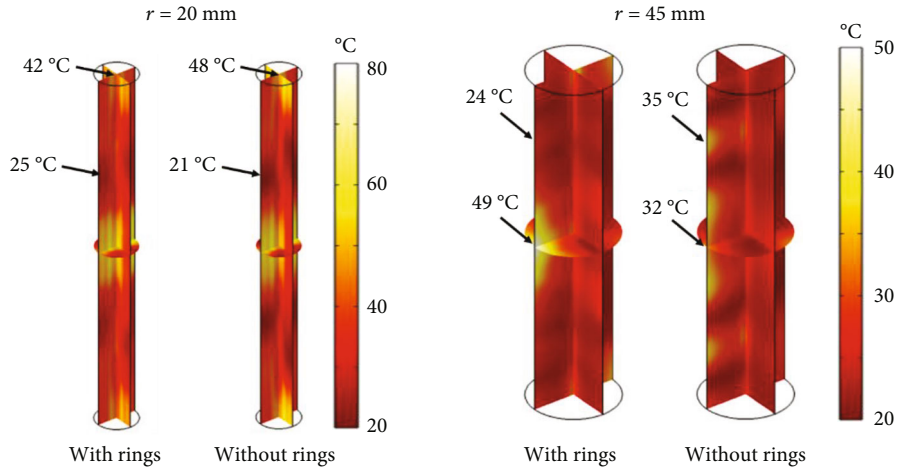

FIGURE 16: Temperature distribution of load with radii of 20 mm and 45 mm.

the inner wall size of the resonant ring change with the radius of the load.

It can be seen from Figure 15 that the radius of the cylindrical load has a strong influence on S_{11} and COV. The heating efficiency of the cylindrical load first increases and then decreases with the radius. When the radius is 40 mm, the energy efficiency of the microwave is the highest. Using resonant rings can slightly increase the heating efficiency and reduce S_{11} by about 2 dB. In addition, the use of the resonant rings can reduce the COV when the load radius is less than 40 mm. When the radius of the load is greater than 40 mm, the resonance rings cannot be used to improve the uniformity of heating. The reason for this phenomenon is related to whether there is a thermal focusing phenomenon in the cylindrical load. When the size of the load is too large, the microwave can only act on the surface of the load, and hot spots will appear on the surface. Since the hot spots brought by the resonant rings are also on the surface, the uniformity of heating may deteriorate. Then, the temperature distribution of the cylindrical load is analyzed when the radius is 20 mm and 40 mm, as shown in Figure 16. When the load radius is 20 mm, thermal focus occurs inside the load, and the resonant ring makes the thermal focus no longer significant. While the load radius is 40 mm, the hot spots are distributed on the surface, so the effect of the rings to improve the uniformity is not obvious. Therefore, it can be concluded that the use of resonant rings can improve heating efficiency, although not very obvious. At the same time, the use of resonant rings is limited, and it is suitable for load sizes that are prone to thermal focus.

Based on this model, the heating uniformity and efficiency of loads with different relative permittivities are analyzed. The real part of the relative permittivities of the load ranges from 20 to 80 with an increment of 10, and the dielectric loss tangents are 0.1 and 0.2, respectively. The simulation results of S_{11} and COV are shown in Figure 17. It is indicated that the use of resonant rings always has the effect of increasing the heating efficiency for loads with different permittivities. The relative permittivity of the load has a great influence on the heating uniformity because it determines the focus position of the microwave inside the load. The simulation results in Figure 17 can help explain the discrepancies between the experimental and simulation results in Figure 7. Using the resonant ring, the change of COV

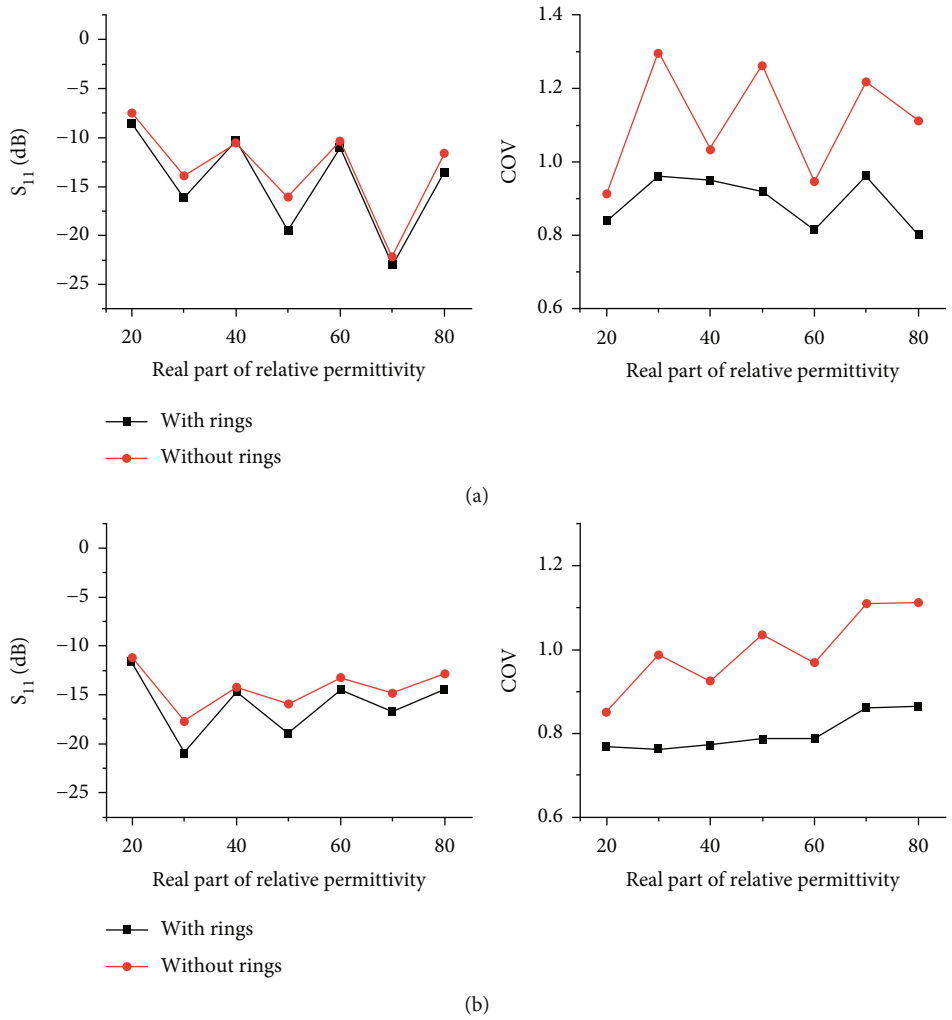

Figure 17: Comparison of S_{11} and COV with different relative permittivities. (a) The electromagnetic loss tangent is 0.1. (b) The electromagnetic loss tangent is 0.2.

with the relative permittivity is not obvious, and the curve remains relatively stable. Using the resonant rings makes it possible to reduce the COV value by a maximum of 0.3. It can also be seen from the simulation results that the larger the dielectric loss tangent, the higher the energy efficiency of the microwave, and the fluctuation of the COV curve is also weakened. The proposed method improves the efficiency and uniformity of microwave heating, and it is suitable for a wide range of relative permittivity loads.

4. Conclusions

In this paper, the method of employing resonant rings surrounding the cylindrical tube to reduce the thermal focus in the center of the cylindrical loads is proposed. The model of microwave heating with a cylindrical tube is established in COMSOL to compare the heating performance with and without resonant rings. A microwave heating system was built to heat the agar gel. The experimental results are basically in agreement with the simulation results; both showed that the resonant rings can mitigate the thermal focus in the cylindrical load and improve the uniformity of heating. Analysis of the results of the electric field and temperature distribution revealed that the resonant ring generated high-order modes of the electromagnetic field in the cavity, thus making microwave heating more uniform. Meanwhile, the influence of the number of resonant rings on the heating uniformity is discussed. The temperature uniformity of the load is improved with the increase in the number of resonant rings. When employing 9 resonant rings, the COV decreased from 1.064 to 0.793. Moreover, the effect of load parameters on heating was analyzed. The radius of the load will affect the focus of the microwave. When the radius of the cylindrical load is greater than 40 mm, the hot spots of the microwave are distributed on the surface of the cylinder. At this time, the improvement of the uniformity of the resonant ring is not obvious. When the cylinder radius is less than 40 mm, the use of resonant rings can significantly improve the uniformity of heating. The proposed method is suitable for cylindrical loads with different permittivities to improve heating uniformity. This work helps to promote the development of microwave energy in industrial applications, especially in the continuous production of materials.

Data Availability

The data are available from the corresponding author upon reasonable request.

Conflicts of Interest

The authors declare no conflict of interest.

Acknowledgments

This study was supported by the National Natural Science Foundation of China (61971295), Nature Science Foundation of Sichuan Province (2022NSFSC0562), and National Key Project (GJXM92579).

References

[1] D. Adam, "Microwave chemistry: out of the kitchen," *Nature*, vol. 421, no. 6923, pp. 571-572, 2003.

[2] M. Huang, E. Xiong, Y. Wang et al., "Fast microwave heating-based one-step synthesis of DNA and RNA modified gold nanoparticles," *Nature Communications*, vol. 13, no. 1, p. 968, 2022.

[3] Y. Mohtashami, S. C. Hagness, and N. Behdad, "A hybrid slot/monopole antenna with directional heating patterns for microwave ablation," *IEEE Transactions on Antennas and Propagation*, vol. 65, no. 8, pp. 3889–3896, 2017.

[4] H. Zhu, J. Su, F. Yang et al., "Effect of lossy thin-walled cylindrical food containers on microwave heating performance," *Journal of Food Engineering*, vol. 337, p. 111232, 2023.

[5] Q. Guo, D. W. Sun, J. H. Cheng, and Z. Han, "Microwave processing techniques and their recent applications in the food industry," *Trends in Food Science and Technology*, vol. 67, pp. 236–247, 2017.

[6] P. Coronel, J. Simunovic, and K. P. Sandeep, "Temperature profiles within milk after heating in a continuous-flow tubular microwave system operating at 915 MHz," *Journal of Food Science*, vol. 68, no. 6, pp. 1976–1981, 2003.

[7] A. Z. Fia and J. Amorim, "Heating of biomass in microwave household oven - a numerical study," *Energy*, vol. 128, article 119472, 2020.

[8] H. Zhang and A. K. Datta, "Heating concentrations of microwaves in spherical and cylindrical foods," *Food and Bioproducts Processing*, vol. 83, no. 1, pp. 14–24, 2005.

[9] N. Soto-Reyes, A. L. Temis-Pérez, A. López-Malo, R. Rojas-Laguna, and M. E. Sosa-Morales, "Effects of shape and size of agar gels on heating uniformity during pulsed microwave treatment," *Journal of Food Science*, vol. 80, no. 5, pp. 1021–1025, 2015.

[10] A. Bresciani, D. Erba, M. C. Casiraghi, S. Iametti, A. Marti, and A. Barbiroli, "Pasta from red lentils (Lens culinaris): the effect of pasta-making process on starch and protein features, and cooking behavior," *Food*, vol. 11, no. 24, p. 4040, 2022.

[11] H. Topcam and F. Erdogdu, "Designing system cavity geometry and optimizing process variables for continuous-flow microwave processing," *Food and Bioproducts Processing*, vol. 127, pp. 295–308, 2021.

[12] A. Rafe, T. Shadordizadeh, M. Hesarinejad et al., "Effects of concentration and heating/cooling rate on rheological behavior of Sesamum indicum seed hydrocolloid," *Food*, vol. 11, no. 23, p. 3913, 2022.

[13] R. Morschhäuser, M. Krull, C. Kayser et al., "Microwave-assisted continuous-flow synthesis on industrial scale," *Green Processing and Synthesis*, vol. 1, no. 3, pp. 281–290, 2012.

[14] M. R. Hossan, D. Y. Byun, and P. Dutta, "Analysis of microwave heating for cylindrical shaped objects," *International Journal of Heat and Mass Transfer*, vol. 53, no. 23-24, pp. 5129–5138, 2010.

[15] Y. Wang, X. Yang, and Y. Qiu, "Double pendulum mode stirrer for improved multimode microwave heating performance," *International Journal of RF and Microwave Computer-Aided Engineering*, vol. 31, no. 11, Article ID e22866, 2021.

[16] H. Zhu, Y. H. Liao, W. Xiao, J. H. Ye, and K. M. Huang, "Transformation optics for computing heating process in microwave applicators with moving elements," *IEEE Transactions on Microwave Theory and Techniques*, vol. 65, no. 5, pp. 1434–1442, 2017.

[17] J. L. Pedreño-Molina, J. Monzó-Cabrera, and J. M. Catalá-Civera, "Sample movement optimization for uniform heating in microwave heating ovens," *International Journal of RF and Microwave Computer-Aided Engineering*, vol. 17, no. 2, p. 152, 2007.

[18] C. Wang, W. Yao, H. Zhu, Y. Yang, and L. Yan, "Uniform and highly efficient microwave heating based on dual-port phase-difference-shifting method," *International Journal of RF and Microwave Computer-Aided Engineering*, vol. 31, no. 9, Article ID e22784, 2021.

[19] M. Li, X. Wu, D. Han et al., "A high-efficiency single-mode traveling wave reactor for continuous-flow processing," *Processes*, vol. 10, no. 7, p. 1261, 2022.

[20] M. Bhattacharya and T. Basak, "A Galerkin finite element based analysis on the microwave heating characteristics of lossy samples in the presence of low and high lossy containers," *International Journal of Heat and Mass Transfer*, vol. 153, p. 119544, 2020.

[21] M. Bhattacharya and T. Basak, "Can the container-dielectrics control heating patterns for microwave assisted material processing? A finite element based introspection," *International Journal of Heat and Mass Transfer*, vol. 205, article 123684, 2023.

[22] S. Tuta and K. Palazoğlu, "Finite element modeling of continuous-flow microwave heating of fluid foods and experimental validation," *Journal of Food Engineering*, vol. 192, pp. 79–92, 2017.

[23] E. Coskun, S. Ozturk, H. Topcam et al., "Continuous-flow microwave processing of peanut butter: a (hypothetical) computational process design study with experimental validation," *Innovative Food Science & Emerging Technologies*, vol. 82, article 103184, 2022.

[24] H. Zhu, J. Ye, T. Gulati et al., "Dynamic analysis of continuous-flow microwave reactor with a screw propeller," *Applied Thermal Engineering*, vol. 123, pp. 1456–1461, 2017.

[25] C. Xu, J. Lan, J. Ye, Y. Yang, K. Huang, and H. Zhu, "Design of continuous-flow microwave reactor based on a leaky waveguide," *Chemical Engineering Journal*, vol. 452, article 139690, 2023.

[26] H. Zhang and A. K. Datta, "Heating concentrations of microwaves in spherical and cylindrical foods: part one: in plane waves," *Food and Bioproducts Processing*, vol. 83, no. 1, pp. 6–13, 2005.

[27] M. Born, *Principles of Optics*, Cambridge University Press, Cambridge, UK, 7th edition, 1999.

[28] Y. Cheng, N. Sakai, and T. Hanzawa, "Effects of dielectric properties on temperature distributions in food model during microwave heating," *Food Science and Technology International*, vol. 3, no. 4, pp. 324–328, 1997.

[29] G. Xiong, H. Zhu, K. Huang, Y. Yang, Z. Fan, and J. Ye, "The impact of pins on dual-port microwave heating uniformity and efficiency with dual frequency," *Journal of Microwave Power and Electromagnetic Energy*, vol. 54, no. 2, pp. 83–98, 2020.